Optical properties and chemical composition of aerosol particles at an urban location: An estimation of the aerosol mass scattering and absorption efficiencies

G. Titos,[1,2] I. Foyo-Moreno,[1,2] H. Lyamani,[1] X. Querol,[3] A. Alastuey,[3] and L. Alados-Arboledas[1,2]

Received 2 August 2011; revised 15 December 2011; accepted 16 December 2011; published 22 February 2012.

[1] We investigated aerosol optical properties, mass concentration and chemical composition over a 1 year period (from March 2006 to February 2007) at an urban site in Southern Spain (Granada, 37.18°N, 3.58°W, 680 m above sea level). Light-scattering and absorption measurements were performed using an integrating nephelometer and a MultiAngle Absorption Photometer (MAAP), respectively, with no aerosol size cut-off and without any conditioning of the sampled air. PM_{10} and PM_1 (ambient air levels of atmospheric particulate matter finer than 10 and 1 microns) were collected with two high volume samplers, and the chemical composition was investigated for all samples. Relative humidity (RH) within the nephelometer was below 50% and the weighting of the filters was also at RH of 50%. PM_{10} and PM_1 mass concentrations showed a mean value of 44 ± 19 $\mu g/m^3$ and 15 ± 7 $\mu g/m^3$, respectively. The mineral matter was the major constituent of the PM_{10-1} fraction (contributing more than 58%) whereas organic matter and elemental carbon (OM+EC) contributed the most to the PM_1 fraction (around 43%). The absorption coefficient at 550 nm showed a mean value of 24 ± 9 Mm^{-1} and the scattering coefficient at 550 nm presented a mean value of 61 ± 25 Mm^{-1}, typical of urban areas. Both the scattering and the absorption coefficients exhibited the highest values during winter and the lowest during summer, due to the increase in the anthropogenic contribution and the lower development of the convective mixing layer during winter. A very low mean value of the single scattering albedo of 0.71 ± 0.07 at 550 nm was calculated, suggesting that urban aerosols in this site contain a large fraction of absorbing material. Mass scattering and absorption efficiencies of PM_{10} particles exhibited larger values during winter and lower during summer, showing a similar trend to PM_1 and opposite to PM_{10-1}. This seasonality is therefore influenced by the variations on PM composition. In addition, the mass scattering efficiency of the major aerosol constituents in PM_{10} were also calculated applying the multilinear regression (MLR) analysis. Among all of them, the most efficient in terms of scattering was sulfate ion (7 ± 1 m^2g^{-1}) while the least efficient was the mineral matter (0.2 ± 0.3 m^2g^{-1}). On the other hand, we found that the absorption process was mainly dominated by carbonaceous particles.

Citation: Titos, G., I. Foyo-Moreno, H. Lyamani, X. Querol, A. Alastuey, and L. Alados-Arboledas (2012), Optical properties and chemical composition of aerosol particles at an urban location: An estimation of the aerosol mass scattering and absorption efficiencies, *J. Geophys. Res.*, *117*, D04206, doi:10.1029/2011JD016671.

1. Introduction

[2] In recent years, interest in better understanding the factors affecting the Earth's radiation budget, and hence the global climate has increased considerably. The global mean radiative forcing (RF) due to aerosol particles has been estimated to be -0.5 ± 0.4 W m^{-2} [*Forster et al.*, 2007]. *Ramanathan and Carmichael* [2008] inferred a RF of +0.9 W m^{-2} for current black carbon levels (more than half the value of the current CO_2 forcing). Air pollutants that form scattering aerosols with negative RF (e.g., sulfate, nitrate, and organic carbon) and absorbing aerosols with positive RF (e.g., black carbon) affect the radiation budget in the opposite way [*Kopp and Mauzerall*, 2010]. The direct radiative forcing of aerosols is often expressed through their different chemical components, making the chemical composition one of the most important parameter for determining the climate role of aerosols. To estimate their impact, several

[1]Centro Andaluz de Medio Ambiente, Junta de Andalucía and Universidad de Granada, Granada, Spain.
[2]Departamento de Física Aplicada, Universidad de Granada, Granada, Spain.
[3]IDÆA, Department of Geosciences, CSIC, Barcelona, Spain.

0148-0227/12/2011JD016671

key parameters are required as the aerosol light scattering and absorption coefficients (σ_{sca} and σ_{abs}, respectively), aerosol single scattering albedo (ω_0) and mass concentration.

[3] The mass scattering and absorption efficiencies (α_{sca}; α_{abs}) of different aerosol chemical species are the key parameters used to connect aerosol chemical properties and radiation models [*Seinfeld and Pandis*, 1998]. The α_{sca} (α_{abs}) is determined using concurrent measurements of the aerosol σ_{sca} (σ_{abs}) and particle mass. Although several studies have estimated the mass scattering and absorption efficiencies in the last decade, most of them are limited to specific periods of the year (field campaigns) and/or are carried out in remote areas. *Hand and Malm* [2007] emphasized the importance of performing measurements over an extended period of time to obtain representative estimations of mass scattering efficiencies due to their importance in climate models. Moreover, many previous derivations of α_{sca} have been made using only sulfate to represent particle mass [*Vrekoussis et al.*, 2005; *Bryant et al.*, 2006], and other components, such as mineral matter, nitrate or organic aerosols, were not considered. This assumption is not valid and it is clear that other aerosols species play an important role in the scattering process [*Andreae et al.*, 2002; *Hand and Malm*, 2007; *Cheng et al.*, 2008].

[4] Measurements of the aerosol optical properties are relatively scarce, especially in the Iberian Peninsula, while most monitoring stations determine PM_{10}, $PM_{2.5}$ and/or PM_1. Therefore, the mass scattering and absorption efficiencies could be used to determine optical properties from PM measurements. In this sense, the goal of this work is to obtain representative estimations of mass scattering and absorption efficiencies of the major aerosol constituents. Different methods have been applied for the computation of scattering and absorption efficiencies, some of them consider the bulk aerosol mass while others try to offer some discrimination using chemical speciation and size segregation [*Formenti et al.*, 2001; *Andreae et al.*, 2002; *Vrekoussis et al.*, 2005; *Hand and Malm*, 2007]. In this work we discuss about the results of these different methods with the objective of gaining knowledge about the aerosol in our urban environment. For this purpose, both optical and chemical properties of atmospheric aerosols in Granada, Spain, from March 2006 to February 2007 are presented. Measurements include PM_{10} and PM_1 mass concentrations and their chemical speciation, aerosol light scattering and absorption coefficients, single scattering albedo and scattering Angström exponent. Connections between the parameters mentioned above are also analyzed. *Lyamani et al.* [2010] presented a comprehensive study of the physical properties of the urban aerosol at Granada, covering two years of data and using different temporal intervals. Although seasonal, weekly and daily behavior of the urban aerosol from the physical point of view were analyzed in detail previously, in the present paper the optical properties are interpreted based in the comparison with aerosol chemical composition.

2. Experimental Site

[5] The measurements presented in this study were performed at an urban site, Granada, from March 2006 to February 2007. Granada (37.18°N, 3.58°W, 680 m a.s.l) is located in southeastern Spain and is a non-industrialized medium-sized city. Near continental conditions prevailing at this site are responsible for large seasonal temperature differences. Most rainfall occurs during winter and spring.

[6] The measurement station is located in the southern part of the city and is less than 500 m away from a highway that surrounds the city. The local aerosol sources are mainly road traffic (dominated by diesel engines) together with soil re-suspension, especially during the warm-dry season when the reduced rainfall may increase the contribution of local mineral dust [*Lyamani et al.*, 2010]. During winter, domestic heating (based on fuel oil combustion) represents an additional source of anthropogenic aerosols.

3. Instrumentation and Methodology

3.1. Optical Aerosol Measurements

[7] Air sampling for all the optical instruments was obtained from the top of a stainless steel tube, 20 cm diameter and 5 m length [*Lyamani et al.*, 2008, 2010]. The inlet is located about 15 m above the ground. Measurements were performed neither with aerosol size cut-off and heating of sampled air. Inside the tube, there are several stainless steel pipes that drive the sampling air to the different instruments. Each one of the stainless pipes extracts the appropriate flow for each instrument. Different diameters of the pipes have been selected in order to optimize the efficiency of the system [*Baron and Willeke*, 2001].

[8] Aerosol scattering coefficient (σ_{sca}) was measured with an integrating nephelometer (TSI, model 3563) at three wavelengths 450, 550 and 700 nm. This instrument draws the ambient air through at a flow rate of 30 l min^{-1}, illuminates the sample with a halogen lamp and measures scattered light at 450, 550 and 700 nm. Calibration of the nephelometer was carried out every three months using CO_2 and filtered air. In this study, non-idealities due to truncation errors were corrected [*Anderson and Ogren*, 1998].

[9] *Zieger et al.* [2011] showed that the increase in the scattering coefficient due to the effect of relative humidity is almost negligible for RH below 50%. In addition, the World Meteorological Organization Global Atmosphere Watch recommends for aerosol monitoring stations to keep sample air RH at 45 $\pm$ 5% [*World Meteorological Organization*, 2003]. In our case, although no drying of the aerosol stream was performed, the relative humidity measured within the nephelometer chamber presented a mean value of 28 $\pm$ 7%, ranging between 8 and 50%. The 99th and 90th percentiles were 42.5 and 37.4%, respectively. Thus, we can consider that the hygroscopic growth does not affect significantly our measurements.

[10] The aerosol light-absorption coefficient, σ_{abs}, was measured with a MultiAngle Absorption Photometer (MAAP) at 637 nm [*Müller et al.*, 2011]. A detailed description of the method is provided by *Petzold and Schönlinner* [2004]. The MAAP draws the ambient air at constant flow rate of 16.7 l min^{-1} and provides 1 min values. No corrections were applied to the data.

3.2. PM Sampling and Chemical Analysis

[11] Two high-volume samplers (flow rate 30 m^3 h^{-1}) were used for sampling PM_{10} (CAV-A/MSb) and PM_1 (Digitel DHA-80) using quartz fiber filters. The filters were conditioned and treated pre- and post-sampling. Filters were

placed in desiccators for 48 h prior to weighing. The weighing room was stabilized at 23°C and 50% RH.

[12] Once the PM mass concentrations were determined by gravimetry, the filters experienced different laboratory treatments for determining the levels of major and trace components following the procedure of *Querol et al.* [2009]. A fraction of each filter of approximately 150 cm^2 was acid digested (HF HNO_3:$HClO_4$, 5:2.5:2.5 ml), kept at 90°C in a Teflon reactor for 6 h, driven to dryness and re-dissolved with 2.5 ml HNO_3 to make up a volume of 50 ml with Milli-Q grade water for the chemical analysis. Inductively Coupled Plasma Atomic Emission Spectrometry (ICP-AES: IRIS Advantage TJA Solutions, THERMO) was used for the determination of the major and some trace elements and Mass Spectrometry (ICP-MS: X Series II, THERMO) for the trace elements. For quality control of the analytical procedure a small amount (approximately 15 mg) of the NIST - 1633b (fly ash) reference material loaded on a similar fraction of blank quartz filter was also analyzed. After blank concentrations were subtracted, analytical errors were <10% for most elements, with the exception of P and K (<15%). Another fraction of filter of about 75 cm^2 was water leached with deionized water (30 g of Milli-Q grade water) to extract the soluble fraction. The solution obtained was analyzed by ion chromatography for determination of Cl^-, SO_4^{2-}, and NO_3^-, and by colorimetry –Flow Injection Analysis (FIA) for NH_4^+. A third portion of filter of around 1 cm^2 was used to determine total carbon content using a LECO [*Querol et al.*, 2004]. SiO_2 and CO_3^{2-} were indirectly determined on the basis of empirical factors (SiO_2 = 3 × Al_2O_3 and CO_3^{2-} = 1.5xCa + 2.5xMg [*Querol et al.*, 2004]). Marine sulfate (SO_4^{2-}m) concentration was determined from the Na concentration according to the Na/SO_4^{2-} molar ratio observed in seawater [*Drever*, 1982]. The difference between total sulfate and marine sulfate is named as non marine sulfate (SO_4^{2-}nm). The non mineral carbon (C_{nm}) was estimated by subtracting the C associated to the carbonates from the total carbon. Then, organic matter and elemental carbon (OM+EC) levels were estimated by applying a factor of 1.4 [*Turpin et al.*, 2000] to on half of the concentrations of C_{nm} (assuming OC is 1/2 C_{nm} and EC is 1/2 C_{nm}). The percentage of mass determined with respect the total PM mass was in average 95% for PM_{10} and 82% for PM_1. The remaining undetermined mass is attributed to the structural and adsorbed water that was not removed during the sample conditioning.

[13] PM components were grouped as: mineral (Σ Al_2O_3, SiO_2, CO_3, Ca, Fe, Mg, K), secondary inorganic aerosols (SIA, Σ SO_4^{2-}nm, NO_3^-, NH_4^+), sea spray (Σ Na, Cl, SO_4^{2-}m), metals (ΣLi, P, Sc, Ti, V, Cr, Mn, Co, Ni, Cu, Zn, Ga, Ge, As, Se, Rb, Sr, Cd, Sn, Sb, Cs, Ba, La, Ce, Lu, Hf, Ta, W, Tl, Pb, Bi, Th and U) and organic matter and elemental carbon (OM+EC).

[14] The sampling period was 24 h starting at 7:00 GMT. During most of the study period, the sampling was carried out each 4 days in order to obtain a homogenous sampling. A total of 62 PM_{10} and 66 PM_1 daily samples were collected following the procedure described above with 55 of them simultaneously collected. Furthermore, a total of 47 24 h periods were available with simultaneous measurements of the integrating nephelometer, the MAAP and the two high-volume samplers. Both the scattering and the absorption coefficients were averaged over the sampling periods.

3.3. Data Treatment

[15] In addition to the direct measurements obtained with the above detailed instrumentation, the scattering Angström exponent (a), which characterizes the wavelength dependence of σ_{sca} was calculated according to the following formula for λ_1 = 700 nm and λ_2 = 450 nm.

$$a_{\lambda_1-\lambda_2} = -(\log\sigma_{sca}(\lambda_1) - \log\sigma_{sca}(\lambda_2))/(\log\lambda_1 - \log\lambda_2) \quad (1)$$

The Angström exponent increases with decreasing particle size and takes values around 2 when the scattering process is dominated by fine particles, while it is close to 0 when the scattering process is dominated by coarse particles [*Seinfeld and Pandis*, 1998; *Schuster et al.*, 2006].

[16] The single scattering albedo (ω_0) represents a key parameter in describing aerosol optical properties. This parameter is defined as the ratio between the scattering and the extinction coefficients at a given wavelength,

$$\omega_0(\lambda) = \sigma_{sca}(\lambda)/\sigma_{ext}(\lambda) \quad (2)$$

To determine ω_0 at 550 nm we have calculated σ_{abs} at 550 nm using the absorption coefficient at 637 nm measured with MAAP and Angström exponent value of 1 that is considered appropriate for an urban atmosphere where black carbon (mainly emitted by vehicles) is the main light absorber [*Kirchstetter et al.* 2004].

[17] The simultaneous measurements of aerosol mass concentration and scattering/absorption coefficients allowed the estimation of the mass scattering/absorption efficiencies. There are four basic approaches to estimate α_{sca} and α_{abs} [*Hand and Malm*, 2007]: (1) *Theoretical Method* consists in the application of Mie calculation based on measurements of size distributions of particle mass or number concentration and assumed refractive index [*Ouimette and Flagan*, 1982; *White*, 1986; *Lowenthal et al.*, 1995]; (2) *Partial Scattering Method* estimates the change in extinction due to the removal or addition of a single species [*Lowenthal et al.*, 1995]; (3) *Measurement Method* defines the mass scattering efficiency of an aerosol population as the ratio of the scattering coefficient corresponding to the mass concentration of that population; (4) *Multilinear Regression* (MLR) method consists in a multiple linear regression with measured scattering or absorption coefficients as the independent variable and measured mass concentrations for each species as the dependent ones [*White et al.*, 1994; *Lowenthal et al.*, 1995; *Formenti et al.*, 2001; *Andreae et al.*, 2002]. Due to the data available both the measurement and MLR methods were applied. Many authors have reported the limitations and requisites of MLR method [*Ouimette and Flagan*, 1982; *White*, 1986; *Lowenthal et al.*, 1995; *Vasconcelos et al.*, 2001; *Hand and Malm*, 2007]. The assumptions required in this method are that all the aerosol species contributing to extinction are included in the model and that the concentrations of the species are uncorrelated. In addition, the number of samples has to be large enough in order to obtain stable solutions. The mass efficiencies derived with this method are subject to a variety of errors. For example, for species with lower measurement uncertainties (e.g., sulfate) the coefficients obtained can be artificially high, while for species with larger measurement uncertainties (e.g., organic matter) may be too low [*White*

and Macias, 1987]. Furthermore, the apportionment of scattering by more than one species to total scattering depends on whether the aerosols are externally or internally mixed [*White*, 1986]. In this sense, when assuming an internal mixture the efficiencies obtained correspond only to the specific mass efficiencies of the mixed aerosol. Regarding the measurement method, the mass efficiencies derived also correspond to the specific mass efficiencies of the mixed aerosol and represent average conditions of an aerosol that could be changing because of variations (such as meteorology or composition) during the sampling period. This is the simplest method for computing mass efficiencies and can be performed when no speciation or size resolved data are available.

4. Results and Discussion

4.1. PM_{10} and PM_1 Levels and Chemical Speciation

[18] During the study period, the average PM_{10} mass concentration was 44 ± 19 $\mu g/m^3$ which is slightly higher than the annual mean value limit (40 $\mu g/m^3$) established by European Directives (2008/30/CE). If the days with African dust outbreaks are not taken into account, the annual limit value was reduced down to 37 ± 13 $\mu g/m^3$. The daily limit value (DLV) of 50 $\mu g/m^3$ fixed by this directive was exceeded in 20 occasions; 14 of them occurring under African dust intrusions (www.calima.ws). Since the number of measurements was reduced to around 15% of the days of the year, this number of exceedances cannot be compared with the number of exceedances of the daily limit value, maximum of 35 days of 365. The Directive 2008/50/CE states that when a low percentage of annual data coverage is available, and provided that the data available is distributed across the whole year, to evaluate compliance with the daily limit value, the 50 $\mu gPM_{10}/m^3$ value as maximum value for the 90.4 percentile of the data set should be used instead of the number of allowed daily exceedances. In our case, the daily limit value is clearly exceeded (by obtaining a percentile 90.4 of 68 $\mu gPM_{10}/m^3$), even when excluding days with African outbreaks (percentile 90.4 of 54 $\mu gPM_{10}/m^3$).

[19] The average PM_{10} mass concentration measured in our station was higher than the annual mean value of 38 ± 15 $\mu g/m^3$ found in the urban background station BCN-CSIC (Barcelona, Spain) during 2007 by *Pérez et al.* [2010]. However, the mean PM_1 mass concentration (15 ± 7 $\mu g/m^3$, same value when excluding African days) was slightly lower than the one obtained at BCN-CSIC station (17 ± 8 $\mu g/m^3$). In spite of the difference in the city size, and road traffic volume, PM_{10} levels in Granada are higher than in Barcelona because: (1) Granada is very influenced with a higher frequency by Saharan air masses and dryness of the terrain also favors the re-suspension of material from the ground (which is mainly in the coarse fraction); (2) The orography of Granada favors the accumulation of urban pollutants. Although PM sources are often local, a fraction of PM_1 may be related to regional and long range transport. This may be particularly important in summer in the Mediterranean area, where ammonium sulfate may have a regional origin [*Rodríguez et al.*, 2002; *Querol et al.*, 2009]. The main difference between PM_1 speciation in Granada and Barcelona is that in Granada the mineral mass concentration in the fine fraction is higher. Since Barcelona is a more populated city with more vehicles and industries it would be expected that the PM_1 fraction would be much higher than in Granada.

[20] The PM_{10} levels obtained in our site were within the range observed in other urban areas and curbside stations across Spain by *Querol et al.* [2008] for the period 1999–2005; but slightly higher compared to other European cities [*Putaud et al.*, 2010]. It has to be bearing in mind that the measurement site is located at 15 m above ground, and that at 4 m (as most of the air quality monitoring sites are located), PM levels will increase considerably. Usually, PM_{10} mass concentrations were higher in Southern Europe than in Northwestern and Central Europe and in curbside and urban stations than in other stations [*Querol et al.*, 2008; *Putaud et al.*, 2010].

[21] The coarse (PM_{10-1}) mass concentration was determined as the difference between the PM_{10} and PM_1 mass concentrations (55 simultaneous samples). It presented a mean value of 30 ± 19 $\mu g/m^3$, ranging between 4 and 87 $\mu g/m^3$.

[22] The coarse and fine mass concentrations presented a clear seasonality (Figure 1). The coarse mass concentration was high in spring and summer while the fine mass concentration presented high values in spring and winter. The coarse mass concentration increased during spring and summer due to the dryness of the soil that favors re- suspension processes and the higher likelihood of dust intrusions from the African continent. In fact, the maximum mass concentrations of the coarse fraction were found during these seasons. Due to the high variability of the processes that favor high coarse mass concentrations, standard deviations were also larger in spring and summer than in autumn and winter. On the other hand, the fine mass concentration seasonality is probably related to the increase in the anthropogenic emissions in winter and spring. The topographic and meteorological conditions of Granada also favor the accumulation of particles in these seasons.

[23] To understand the contribution of PM_1 to PM_{10}, the daily variability of the ratio PM_1/PM_{10} is plotted in Figure 2. The decrease of this ratio during summer can be attributed to re-suspension, low precipitation and more frequency of African intrusions [*Pérez et al.*, 2008]. The PM_1/PM_{10} ratio had a mean value of 0.4 ± 0.2, ranging from 0.1 to 0.8, with the highest variability in spring.

[24] Speciation data from PM_{10}, PM_1 and PM_{10-1} fractions is presented in Table 1. Figure 3 shows the contribution of the different compounds to the coarse and fine fractions.

[25] Mineral matter was the major constituent in the PM_{10} fraction with a mean value (±standard deviation) of 19 ± 15 $\mu g/m^3$ (Table 1), contributing more than 43% to this fraction. The mineral matter concentration obtained in this work was larger than those found by *Querol et al.* [2008] at different Spanish stations during the period 1999–2005. The contribution of mineral particles to PM_{10} levels in Granada was slightly higher than the contribution obtained at road side sites (26–36%) and at urban sites in the Iberian Peninsula (20–33%) [*Querol et al.*, 2008]. Lower contributions of mineral particles to the PM_{10} fraction were also reported for urban and curbside stations across Europe [*Putaud et al.*, 2010]. The contribution of this constituent to the fine mode was much smaller (around 10%) than the contribution to the coarse mode (58%), as could be expected since the mineral dust presents a dominant coarse grain size [*Pey et al.*, 2008]. Levels of mineral components in PM_{10-1} have a significant

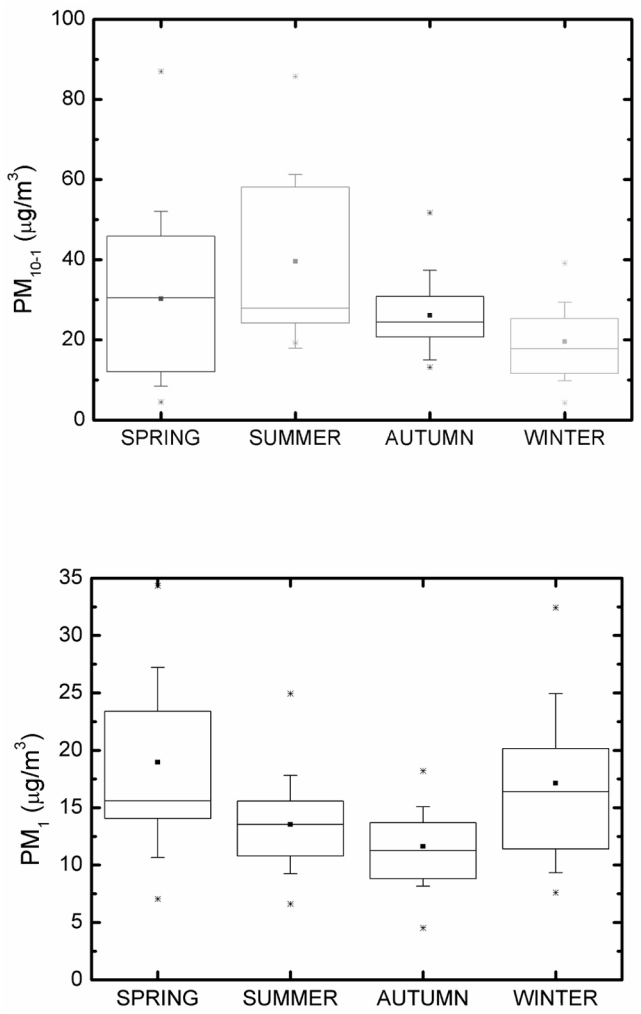

Figure 1. Seasonal variability of the (top) PM_{10-1} and (bottom) PM_1 mass concentrations for the period from March 2006 to February 2007. The error bars are the standard deviation, the box limits are the 25 and 75 percentiles, the mid line is the median and the asterisks are the maximum and minimum values. Spring is March, April and May; Summer is Jun, July and August; Autumn is September, October and November; Winter is December, January and February.

dependency on the traffic activity mainly due to dust re-suspension from the ground, erosion of road pavements and from brake wear [*Amato et al.*, 2009]. So, the high traffic activity in combination with the dryness of the terrain and the scarce rainfall that occurs in Granada could explain the large contribution of mineral particles obtained. Furthermore, dust intrusions from the North African continent are very frequent in Granada (especially in spring and summer) increasing significantly the mineral matter levels and, therefore, PM_{10} levels. During summer, when the re-suspension from the ground is higher and the dust outbreaks are more frequent the mineral matter contributed more than 68% to PM_{10-1} fraction.

[26] The marine components showed very low levels in PM_{10} (1.0 ± 0.6 $\mu g/m^3$) contributing around 2.5% to this fraction. In BCN-CSIC site, sea spray showed slightly higher contributions to PM_{10} fraction (5%) [*Pérez et al.*, 2008] related to its proximity to the Mediterranean Sea. The mean sea spray concentration was in the range 0.7–1.2 $\mu g/m^3$ reported by *Querol et al.* [2008] for inland regions of the Iberian Peninsula.

[27] SIA accounted for around 17% of PM_{10} fraction with a mean value of 8 ± 3 $\mu g/m^3$ (Table 1) and accounted for over 24% of PM_1 fraction. The value obtained in PM_{10} was within the range 6–13 $\mu g/m^3$ reported for urban background stations across the Iberian Peninsula [*Querol et al.*, 2008]. Non marine sulfate was predominantly in the fine fraction, contributing 5.9% and 14.0% to PM_{10-1} and PM_1 fractions, respectively. This component presented a mean concentration in PM_{10} of 4 ± 2 $\mu g/m^3$, which was in the upper end of the range 2–4 $\mu g/m^3$ reported by *Querol et al.* [2004] for non industrialized urban regions. Nitrate levels in PM_{10} (3 ± 2 $\mu g/m^3$) were in the range 1.5–3.9 $\mu g/m^3$ reported by *Querol et al.* [2004] for urban background stations. Similar contributions of nitrate to the coarse and fine fractions (around 6%) were observed. Non marine sulfate, nitrate and ammonium contributions to both, PM_{10} and PM_1 fractions, were lower than those reported by *Pérez et al.* [2008] in Barcelona, denoting the relatively low industrialization level of Granada. Seasonal ionic balance revealed that in winter only 50% of $SO_4^{2-} + NO_3^-$ were neutralized by NH_4^+ while in summer, with a negligible contribution of nitrate, the sulfate was neutralized in a similar fraction.

[28] Organic matter and elemental carbon accounted for around 31% of PM_{10} fraction and for 43% of PM_1 fraction. The OM+EC level in PM_{10} (14 ± 5 $\mu g/m^3$) were in the range 10–15 $\mu g/m^3$ [*Querol et al.*, 2004] and 20–32% [*Querol et al.*, 2008] reported for curbside stations. This constituent is mainly in the fine fraction since its contribution to the coarse fraction (21.5%) is much lower than the contribution to the fine fraction. In the above mentioned studies, high levels of OM+EC were closely correlated with traffic emissions and combustion processes. The contributions of OM+EC particles to both the fine and coarse fractions increased considerably during winter. This fact may be due to the increase in the anthropogenic activity (domestic heating based on fuel-oil combustion) in combination with a

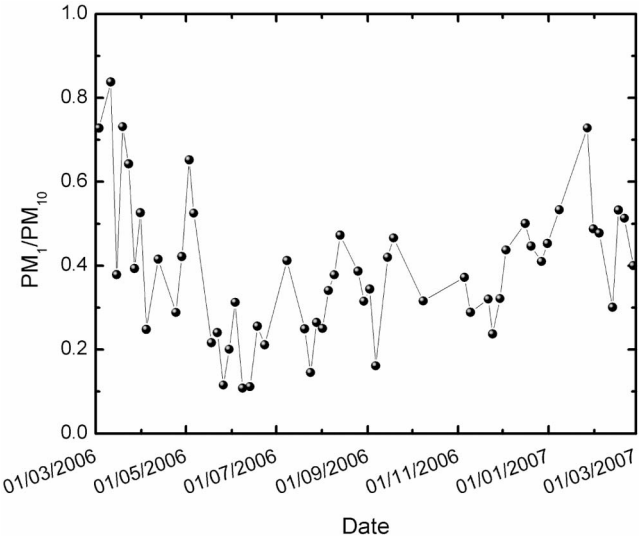

Figure 2. Daily variability of the ratio PM_1/PM_{10}.

Table 1. Basic Statistical Summary of the Mass Concentrations (in $\mu g/m^3$) for the Major Chemical Species Measured in PM_{10}, PM_1 and PM_{10-1} in Granada[a]

	PM_{10} (N = 62)			PM_1 (N = 66)			PM_{10-1} (N = 55)		
	Mean ± SD	Max.	Min.	Mean ± SD	Max.	Min.	Mean ± SD	Max.	Min.
PM	44 ± 19	98	15	15 ± 7	34	5	30 ± 19	87	4
SiO_2	7 ± 7	34	0	0.5 ± 0.5	1.9	0	7 ± 7	34	0
CO_3^{2-}	5 ± 3	15	0	0.3 ± 0.3	1.4	0	4 ± 3	14	0
Al_2O_3	2 ± 2	11	0	0.2 ± 0.2	0.6	0	2 ± 2	11	0
Ca	3 ± 2	10	0	0.2 ± 0.2	0.9	0	3 ± 2	10	0
K	0.8 ± 0.4	1.8	0.2	0.3 ± 0.2	0.9	0.1	0.5 ± 0.3	1.6	0.1
Mg	0.8 ± 0.5	2.2	0.1	0.05 ± 0.05	0.22	0	0.8 ± 0.5	2.2	0.1
Fe	0.9 ± 0.6	3.3	0.1	0.06 ± 0.05	0.22	0	0.9 ± 0.6	3.3	0.1
Na^+	0.5 ± 0.3	1.4	0.1	0.05 ± 0.02	0.1	0.02	0.5 ± 0.3	1.4	0.1
Cl^-	0.4 ± 0.3	1.6	0.0	0.08 ± 0.09	0.46	0.01	0.3 ± 0.3	1.6	0.0
$SO_{4\ m}^{2-}$	0.1 ± 0.1	0.4	0.0	0.01 ± 0.01	0.03	0.0	0.1 ± 0.1	0.4	0.0
$SO_{4\ nm}^{2-}$	4 ± 2	10	2	2 ± 1	5	1	2 ± 1	8	0
NH_4^+	0.6 ± 0.4	1.8	0.1	0.5 ± 0.3	1.6	0	0.1 ± 0.3	1.0	0
NO_3^-	3 ± 2	8	1	1 ± 1	6	0	2 ± 1	5	0
Mineral	19 ± 15	69	2	2 ± 1	6	0	19 ± 15	69	1
OM+EC	14 ± 5	34	6	7 ± 3	21	3	7 ± 3	16	1
Sea Spray	1.0 ± 0.6	3.4	0.3	0.1 ± 0.1	0.5	0.1	0.9 ± 0.6	3.4	0.1
SIA	8 ± 3	15	3	3 ± 2	11	1	4 ± 2	12	1
Metals	0.3 ± 0.2	1.0	0.1	0.05 ± 0.02	0.14	0.01	0.3 ± 0.2	1.0	0
Undetermined	2 ± 4	12	−4.7	4 ± 4	16	−6	−1 ± 4	5	−12

[a]Statistical summary comprises mean value, standard deviation, and maximum and minimum values. Max., maximum; Min., minimum; N, number of samples analyzed.

lower development of the convective mixing layer during winter [*Navas-Guzmán et al.*, 2010] which favors the accumulation of carbonaceous particles emitted by urban sources.

[29] Levels of most trace elements are relatively low when compared with the usual concentration range in urban background environments of Spain reported by *Querol et al.* [2008]. Thus, the typical road traffic tracers such as Cu, Zn, Ba, Sn and Sb; were near three times lower than in large urban agglomerations of Spain. Other environmental relevant elements, such As, Pb, Cd and Cr, were presented in relatively low levels. However, Sr (a crustal component) and V were presented in relatively high concentrations (by a factor of 2 and 1.3 the highest annual mean reported in non industrial urban environments of Spain, [*Querol et al.*, 2008]). Mining and fuel-oil combustion are probably the major sources accounting for this minor geochemical anomaly.

4.2. Analysis of Aerosol Optical Properties

[30] Figure 4 shows the daily variability of the light scattering and absorption coefficients for the period from March 2006 to February 2007. The relative humidity within the nephelometer chamber was below 50%. We have selected those days with simultaneous measurements of light scattering and absorption coefficients and PM_{10} and PM_1 mass concentrations (N = 47). The data represent averages for the same periods over which the aerosol samples were collected. Table 2 presents a statistical summary of the aerosol optical properties obtained during the study period. The mean daily values of σ_{sca}(550 nm)

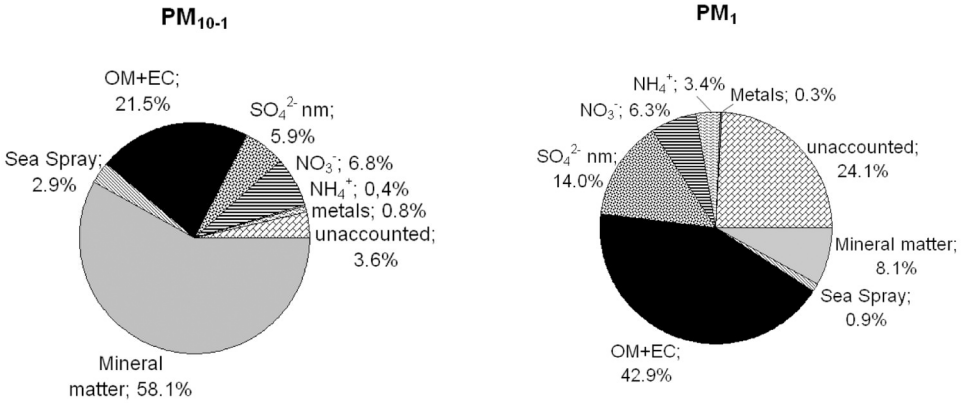

Figure 3. Annual mean composition in % of (left) PM_{10-1} and (right) PM_1 fractions for the period from March 2006 to February 2007.

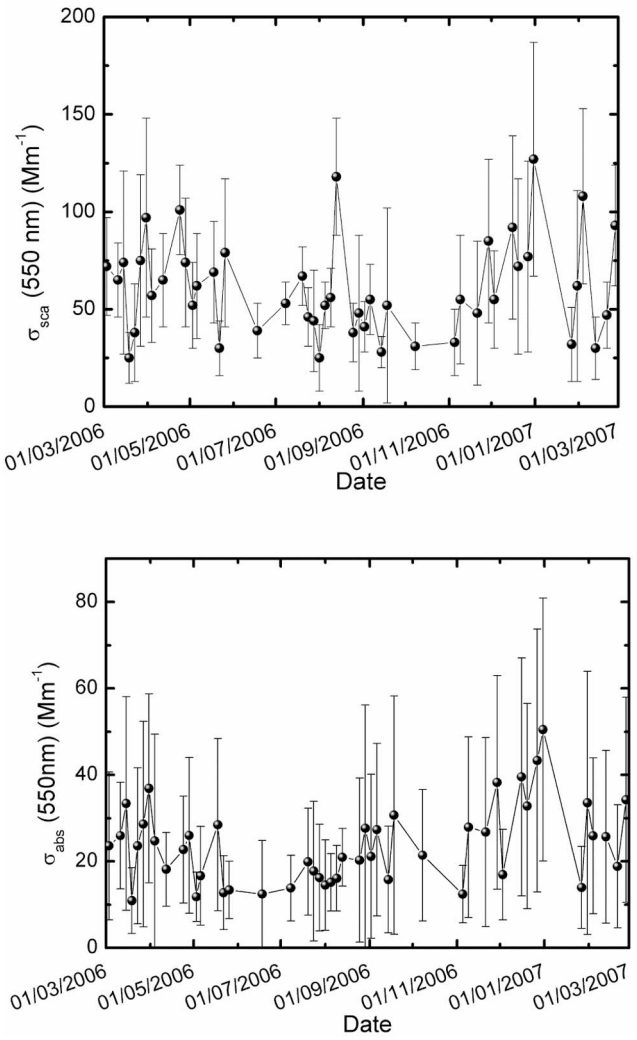

Figure 4. Daily mean value and standard deviation of (top) σ_{sca}(550 nm) and (bottom) σ_{abs}(550 nm) measured at RH < 50%.

ranged between 25 and 128 Mm^{-1} with a mean value and standard deviation of 61 ± 25 Mm^{-1} while σ_{abs}(550 nm) was in the range 11–50 Mm^{-1}, with a mean value of 24 ± 9 Mm^{-1}. These mean values are in accordance with previous results (σ_{sca} (550 nm) = 60 ± 17 Mm^{-1} and σ_{abs}(670 nm) = 21 ± 10 Mm^{-1}) obtained in Granada during a longer study period [*Lyamani et al.*, 2010].

[31] Both the scattering and the absorption coefficients were similar (σ_{sca} = 60 Mm^{-1}; σ_{abs} = 21 Mm^{-1}) to those measured at an urban-coastal site, Toulon (France), during 2005–2006 [*Saha et al.*, 2008]. The average scattering coefficient obtained in this study was larger than those obtained in the Eastern Mediterranean by *Vrekoussis et al.* [2005] (50 ± 23 Mm^{-1} in Finokalia, Greece, and 45 ± 22 Mm^{-1} in Erdemli, Turkey). *Pereira et al.* [2011] calculated in Évora (Portugal) a mean value of σ_{sca}(550 nm) = 43 ± 46 Mm^{-1}, which was also considerably lower than the value obtained in the present study. It can be explained since Évora is a non-polluted small city and Erdemli and Finokalia are remote coastal sites with their highest σ_{sca} values linked to the presence of dust aerosols. A large σ_{sca}(550 nm) of 75 ± 42 Mm^{-1} [*Andreae et al.*, 2002] was estimated at a remote site in the Negev desert of Israel affected by moderately polluted continental air masses.

[32] The scattering coefficient showed a clear seasonal pattern. Large values were found in winter, with a mean value of 70 ± 30 Mm^{-1}, and low in summer (53 ± 24 Mm^{-1}). The same pattern was found for the absorption coefficient, with a mean value of 30 ± 11 Mm^{-1} during winter, while during summer the absorption coefficient presented a mean value of 18 ± 4 Mm^{-1}. Also in winter, the standard deviations were larger than in summer, which could be related to the large day-to-day variability of the atmospheric conditions in winter. During this season, stable anticyclonic conditions that favor accumulation of particles near-surface alternate with the influence of Atlantic air masses that clean the air by advection and/or wet deposition processes. Similar seasonal variations of aerosol scattering and absorption coefficients at our site were also reported by *Lyamani et al.* [2010] from December 2005 to November 2007. These authors attributed this seasonality to seasonal changes in meteorological conditions and emissions.

[33] The scattering Angström exponent ($a_{450–700}$) ranged from 0.6 to 2.2 with an average value of 1.7 ± 0.3. During the study period, this parameter presented values larger than 1.3 in most cases, denoting a predominance of fine particles. The Angström exponent exhibited large values in winter. This fact indicates an increase in the contribution of fine particles during the cold season related with the increase of the anthropogenic activity (domestic heating). As shown in Figure 5 there is a significant negative correlation (R = −0.73) between scattering Angström exponent, $a_{450–700}$, and PM_{10}/PM_1 ratio. In other words, $a_{450–700}$ decreases when the contribution of fine particles to the total mass load decreases. A similar relationship between Angström exponents (column and surface) and the ratio of accumulation mode volume concentration to total volume concentration was reported by *Hand et al.* [2004]. Significant negative correlations have been also observed between Angström exponent and the ratio of C_{nm} in PM_{10}/C_{nm} in PM_1 during winter (R = −0.63) and between Angström exponent and the ratio of mineral matter in PM_{10}/mineral matter in PM_1 during summer (R = −0.69).

[34] The single scattering albedo represents a key parameter in the assessment of the direct effect of atmospheric aerosol particles in the radiative energy budget in terms of their cooling or warming effects. This parameter had a mean value at 550 nm of 0.71 ± 0.07. It presented larger values in spring and summer than in autumn and winter, with a mean value for spring-summer of 0.73 ± 0.06 and for autumn-winter of 0.65 ± 0.06. These results suggest a large contribution of absorbing particles in the study site, which are in accordance with the chemical composition since the contribution of OM+EC (containing absorbing particles) to PM_1

Table 2. Summary of Aerosol Optical Properties[a]

Parameter	Mean ± SD	Median	Min.	Max.	P25	P75
σ_{sca}(550 nm) (Mm^{-1})	61 ± 25	55	25	128	43	74
σ_{abs}(550 nm) (Mm^{-1})	24 ± 9	23	11	50	16	28
ω_0(550 nm)	0.71 ± 0.07	0.71	0.54	0.85	0.66	0.76
$a_{450–700}$	1.6 ± 0.3	1.7	0.6	2.2	1.4	1.9

[a]Aerosol optical properties comprise mean value, standard deviation, median, maximum, and minimum values and 25 and 75 percentiles.

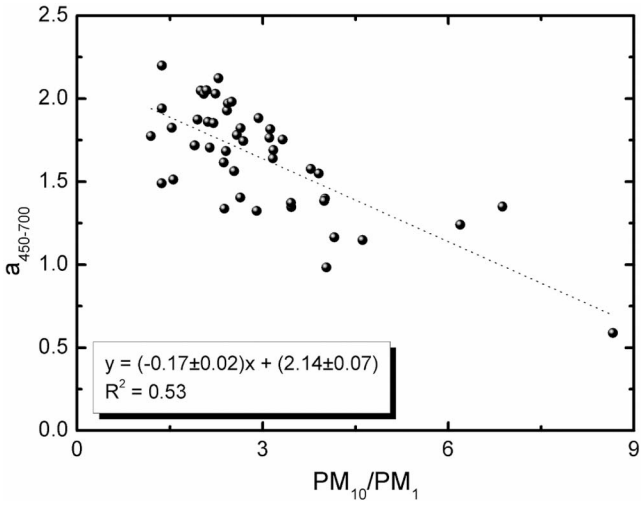

Figure 5. Scattering Angström exponent calculated between 450 and 700 nm versus PM_{10}/PM_1 ratio.

increased from 37.5% in summer to 54.4% in winter. As we mentioned before, the use of domestic heating in conjunction with a lower development of the convective mixing layer could favor the accumulation of carbonaceous particles near surface.

4.3. Mass Scattering and Absorption Efficiencies

4.3.1. Measurement Method

[35] We have applied the measurement method to calculate the mass scattering and absorption efficiencies (α_{sca}; α_{abs}) of the aerosol particles as the ratio between the scattering and the absorption coefficients, respectively, and PM_{10} mass concentration. Since the nephelometer and MAAP do not have size cut-off, we used this method with the PM_{10} mass concentration. As we stated before, the filters were weighted at RH of 50% and the RH within the nephelometer was also below 50%. The RH correction for the mass scattering efficiency requires the assumption of a size distribution in order to compute the f(RH) curves used to "dry out" the scattering efficiency. Regarding the absorption efficiency is known that the effect of the RH on the absorption coefficient is not significant [*Nessler et al.*, 2005]. Thus, due to the measurement conditions we do not consider that corrections are necessary.

[36] During the study period, α_{sca} was in the range 0.6–3.2 m^2g^{-1}, with a mean value of 1.5 ± 0.5 m^2g^{-1}, which was almost three times the value of α_{abs} (0.6 ± 0.2 m^2g^{-1}). The mean α_{sca} obtained in this study was slightly lower than the average value (1.7 ± 1.1 m^2g^{-1}) reported by *Hand and Malm* [2007] for urban regions. A significantly higher value of 2.6 ± 0.8 m^2g^{-1} was estimated at Hyytiälä, Finland [*Virkkula et al.*, 2011], for PM_{10} particles at dry conditions (RH within the nephelometer of 32 ± 11%). *Jung et al.* [2009] obtained at Beijing, for relatively clean conditions, a scattering efficiency for PM_{10} particles of 1.4 ± 0.9 m^2g^{-1}, while for relatively polluted conditions it was 3.1 ± 0.9 m^2g^{-1}.

[37] The seasonal variability of the PM_{10} mass scattering and absorption efficiencies is shown in Table 3. Both of them exhibited larger values in winter (α_{sca} = 2.0 ± 0.5 m^2g^{-1} and α_{abs} = 0.8 ± 0.1 m^2g^{-1}) than in summer (α_{sca} = 1.2 ± 0.4 m^2g^{-1} and α_{abs} = 0.4 ± 0.1 m^2g^{-1}). Similar seasonality in the mass scattering efficiency was obtained in Dongsheng, northern China, by *Yan* [2007]. Although the PM_{10} mass concentration was larger in spring and summer, mainly due to the increase in mineral matter levels, these particles are less efficient in terms of scattering and absorbing radiation, than the aerosol particles that predominate in winter. Thus, mass scattering and absorption efficiencies seasonal patterns are closely related to differences in PM composition. During summer, dust aerosols (mainly coarse grain size) increase their contribution to the PM_{10} fraction while during winter time, OM+EC particles are the major contributors.

4.3.2. Scattering and Absorption Efficiencies for Coarse and Fine Particles Applying MLR Method

[38] The importance of separating between sub- and supermicron particles is clear because these particles have very distinct sources, optical properties, chemical composition and atmospheric lifetime. To derive α_{sca} and α_{abs} of coarse and fine aerosols we have used the following formulas:

$$\sigma_{sca} = \alpha_{sca,C} * [PM_{10-1}] + \alpha_{sca,F} * [PM_1] + I \quad (3)$$

$$\sigma_{abs} = \alpha_{abs,C} * [PM_{10-1}] + \alpha_{abs,F} * [PM_1] + I \quad (4)$$

where σ_{sca} (σ_{abs}) is the aerosol scattering (absorption) coefficient (Mm^{-1}), $\alpha_{sca,C}$ and $\alpha_{sca,F}$ ($\alpha_{abs,C}$ and $\alpha_{abs,F}$) are the mass scattering (absorption) efficiencies of coarse and fine particles, $[PM_{10-1}]$ and $[PM_1]$ are the coarse and fine particulate mass concentrations ($\mu g/m^3$), and I is a constant representing contributions to scattering (absorption) not related to either coarse or fine aerosols (interception with the y axis). The intercept was computed in the regressions; however it is not considered further because it tended to be close to zero and it has no radiative significance.

[39] The coarse and fine mass scattering efficiencies calculated were 0.5 ± 0.2 m^2g^{-1} and 2.5 ± 0.4 m^2g^{-1} (correlation coefficient, R = 0.76), respectively, and the mass absorption efficiency for coarse and fine particles were 0.1 ± 0.1 m^2g^{-1} and 0.8 ± 0.2 m^2g^{-1} (R = 0.62), respectively. So, aerosol particles in the fine mode present higher

Table 3. Seasonal and Annual Mean Values of the PM_{10} Mass Scattering and Absorption Efficiencies for the Period From March 2006 to February 2007

PM_{10} Mass Efficiencies	Spring	Summer	Autumn	Winter	Annual
α_{sca}(550 nm) (m^2g^{-1})	1.5 ± 0.4	1.2 ± 0.4	1.3 ± 0.3	2.0 ± 0.5	1.5 ± 0.5
α_{abs}(550 nm) (m^2g^{-1})	0.5 ± 0.2	0.4 ± 0.1	0.7 ± 0.2	0.9 ± 0.1	0.6 ± 0.2

mass scattering and absorption efficiencies compared to those in the coarse mode denoting that smaller particles extinct light more efficiently at visible wavelengths.

[40] The mass scattering efficiencies obtained in this work were comparable to the values obtained by *White et al.* [1994] in Southwest USA (2.4–2.5 m^2g^{-1} for fine particles and 0.3–0.4 m^2g^{-1} for coarse particles). Very similar values of α_{sca} (2.5 ± 0.6 m^2g^{-1} and 0.6 ± 0.2 m^2g^{-1} for fine and coarse particles, respectively) were also reported by *Chow et al.* [2002] in Tucson (AZ, USA). Furthermore, the α_{sca} obtained in our study were in accordance with the average value proposed by *Hand and Malm* [2007] ($\alpha_{sca,F}$ = 2.3 ± 0.8 m^2g^{-1}; $\alpha_{sca,C}$ = 0.6 ± 0.3 m^2g^{-1}) for urban regions.

[41] Several authors [*Vrekoussis et al.*, 2005; *Bryant et al.*, 2006; *Pandolfi et al.*, 2011] estimated the mass scattering efficiency of fine particles with the measurement method considering that the scattering process was mainly due to particles in the fine mode. Their results were slightly larger than the α_{sca} obtained in this work and than in others that also applied the MLR method, suggesting that the measurement method can overestimate the mass scattering efficiencies derived. To obtain fine mass efficiencies with the measurement method, the total scattering is divided by the PM_1 mass concentration. With this approach, it is necessary to assume that particles in the coarse mode do not contribute to the scattering coefficient. This assumption led to an overestimation just because the total scattering coefficient is attributed to a fraction of the total mass concentration and not to the total mass concentration. It is important to highlight that, although fine particles are more efficient in terms of extinct radiation, it is also necessary to quantify the effect of coarse particles.

4.3.3. Scattering and Absorption Efficiencies for Chemical Species Applying MLR Method

[42] To separate the effects of the different chemical components in the scattering process we have applied different regression models. The MLR analysis has been performed with the total scattering coefficient as the independent variable and the sulfate ion, nitrate, mineral matter, OM+EC and the residual fraction mass concentrations as the dependent ones. To account for the total scattering coefficient the species in the PM_{10} fraction has been used in this analysis. It is remarkable that due to differences in the sampling and analysis methods the obtained efficiencies in different studies are not always directly comparable. For example, differences in the methods used to obtain the chemical composition, in the size cut or in the RH (sampling below 50% or at ambient RH) can contribute to differences in the mass efficiencies obtained. Our estimate of $\alpha_{sca}(SO_4^{2-}\text{nm})$ = 7 ± 1 m^2g^{-1} was in the upper end of the range of values given by *Charlson et al.* [1999]. A similar value of 7 ± 2 m^2g^{-1} was reported for fine sulfate ion by *Formenti et al.* [2001] at the Negev Desert applying the MLR method and with the scattering coefficient measured at RH below 50%. *Vrekoussis et al.* [2005] deduced the mass scattering efficiency for sulfate ion from the slope of the total scattering coefficient versus the SO_4^{2-}nm. They obtained an annual mean value of 5.9 ± 1.7 at Erdemli and 5.7 ± 1.4 m^2g^{-1} at Finokalia. *Pandolfi et al.* [2011] obtained a mean $\alpha_{sca}(SO_4^{2-}\text{nm})$ of 15.6 m^2g^{-1} with a simple linear regression at dry conditions. The mass scattering efficiency obtained for NO_3^- (5 ± 2 m^2g^{-1}) was also above the range of literature values.

[43] The PM_{10} mineral matter mass scattering efficiency obtained in this study (0.2 ± 0.3 m^2g^{-1}) was in the lower end of the range of values reported by *Vrekoussis et al.* [2005] in the Eastern Mediterranean (1 m^2g^{-1} at Finokalia and 0.2 m^2g^{-1} at Erdemli) with the measurement method during dust events. With this same approach, *Pereira et al.* [2008] obtained in Portugal a value of 1.0 ± 0.1 m^2g^{-1}, which was considerably higher than the $\alpha_{sca}(mineral)$ obtained in Granada. A value of 0.9 m^2g^{-1} was estimated for dust aerosols transported from the Sahara desert to Portugal by *Wagner et al.* [2009]. Furthermore, our value was also lower than the values obtained with the MLR method (ranging from 0.5 to 3.1 m^2g^{-1}) by *Hand and Malm* [2007]. It is necessary to remark that the studies we have compared with have been performed during important dust events and that in most cases the use of the measurement method can lead to an overestimation of the α_{sca} calculated. When computing the mineral mass scattering efficiency with the measurement method [*Vrekoussis et al.*, 2005; *Pereira et al.*, 2008; *Wagner et al.*, 2009] the total scattering coefficient is attributed to the mineral mass concentration and, therefore, assuming that other species contribute marginally to the total scattering.

[44] Several authors [*Cheng et al.*, 2008; *Andreae et al.*, 2008] have reported the importance of EC particles in the absorption process, while organic matter (OM) contributes to both, the scattering and the absorption processes. The OM+EC (in PM_{10}) mass scattering efficiency obtained was 2.8 ± 0.4 m^2g^{-1}. We have normalized this value to a carbon multiplier of 1.8 for direct comparisons with other studies. Thus, we obtained a mass scattering efficiency for OM+EC particles of 2.2 m^2g^{-1}. This value was in the range 1.8–4.2 m^2g^{-1} calculated by *Hand and Malm* [2007] for OM particles. *Quinn et al.* [2002] found a OM scattering efficiency of 1.4 m^2g^{-1} at the Indian Ocean applying the MLR method. Our value was closed to that estimated by *Malm and Hand* [2007] for fine (<2.5 μm) OM particles in Phoenix (2.47 m^2g^{-1}) at RH of 0%. These results suggest that EC particles do not contribute significantly to both the scattering coefficient and the total mass load.

[45] In order to validate the mass scattering efficiencies obtained with the MLR model, we have used an extra data set (9 days from April to June 2007) not included in the previous calculation. The scattering coefficient calculated multiplying the mass scattering efficiencies and the corresponding mass concentrations showed a significant correlation (R^2 = 0.89) with the scattering coefficient measured with the nephelometer. Thus, the total scattering coefficient can be derived from PM_{10} speciation using the mass scattering efficiencies.

[46] The MLR method was used to determine the mass absorption efficiencies of the different chemical species as we did to determine the mass scattering efficiencies previously. However, no satisfactory results were found. The C_{nm} was the only species that correlates well with the absorption coefficient, so a simple linear fit has been used in this case (measurement method). Figure 6 shows the absorption coefficient at 550 nm versus C_{nm} mass concentration in PM_{10} and the corresponding linear fit. These parameters exhibit a good correlation (R = 0.94) denoting that carbonaceous matter dominate the absorption process. The C_{nm} absorption efficiency was 1.9 ± 0.1 m^2g^{-1}, considerably

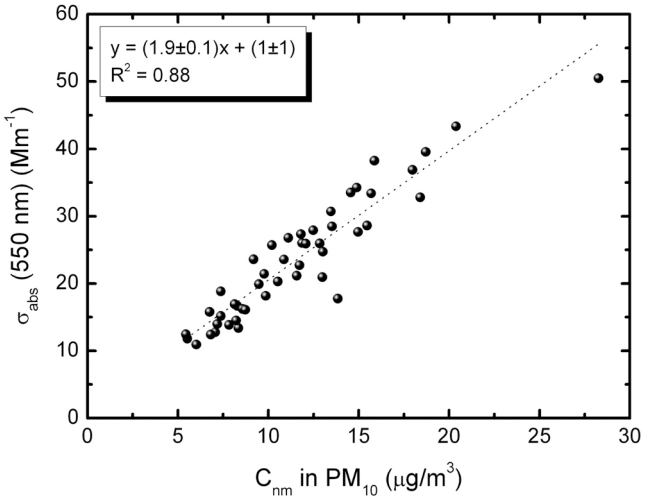

Figure 6. Absorption coefficient at 550 nm versus C_{nm} mass concentration in the PM_{10} fraction and the corresponding linear fit.

lower than the values found in the literature for EC particles [*Bond and Bergstrom*, 2006; *Cheng et al.*, 2008; *Andreae et al.*, 2008; *Pandolfi et al.*, 2011]. This significant difference could be due to the low contribution of OC particles to the absorption process, although these particles contribute significantly to the total C_{nm} mass load.

5. Conclusions

[47] From one year of measurements (from March 2006 to February 2007) performed at an urban site in Southern Spain (Granada), we have estimated different aerosol optical properties, mass concentration and chemical composition. The scattering and absorption coefficients were measured with no aerosol cut-off, and chemical speciation was obtained for PM_{10} and PM_1. The relative humidity within the nephelometer chamber was below 50% and the weighting of the filters was also at this RH. Among all the aerosol constituents, mineral matter (mainly related to re-suspension processes and dust events from North Africa) was the major constituent in the PM_{10-1} fraction while, OM+EC particles (mainly from traffic emissions and combustion processes) contributed the most to the PM_1 fraction. The contribution of mineral matter to the PM_{10} fraction (43%) was larger than those reported for urban and curbside stations around the Iberian Peninsula. Related with this fact, levels of PM_{10} particles were also higher in Granada than in other European cities. Larger PM_{10} concentrations were obtained during summer linked to the increase in the mineral matter levels. In the other hand, the fine mass concentration exhibited large values during spring and winter when the anthropogenic activity is the dominant source.

[48] The total scattering and absorption coefficients presented a mean value of 61 ± 25 Mm^{-1} and 24 ± 9 Mm^{-1}, respectively, showing larger values in winter and lower in summer. Urban aerosols present very low values of single scattering albedo (the mean single scattering albedo at 550 nm in Granada was 0.71 ± 0.07), denoting that these aerosol particles contain a large fraction of absorbing material. In this sense, urban aerosols could affect the radiation budget positively. This effect is very important for the Iberian Peninsula and Europe, moreover taking into account that the world has experienced an unprecedented urban growth in last decades. Furthermore, single scattering albedo seasonality denotes an absorption enhancement during the cold season that could be related to the increase in the anthropogenic activity (levels of OM+EC particles increased considerably during winter) and the predominance of low mixing layer heights at this time of the year. The scattering Angström exponent presented a mean value of 1.7 ± 0.3, suggesting a large fraction of fine particles at this site. Its seasonal variability indicates an increase in the ratio of fine particles during the cold season, an observation confirmed by the PM_1/PM_{10} ratio.

[49] The PM_{10} mass scattering efficiency presented a mean value of 1.5 ± 0.5 m^2g^{-1} (typical of urban areas), which was considerably larger than the PM_{10} mass absorption efficiency. The mass scattering and absorption seasonality show a similar trend to PM_1 and opposite to PM_{10-1}. This seasonality is therefore influenced by the variations on PM composition.

[50] To obtain the contribution of fine and coarse particles to the total scattering and absorption coefficients we applied the MLR method. Although we obtained that fine particles extinct light more efficiently than coarse particles, results suggest that it is also necessary to quantify the effect of coarse particles. The mass scattering and absorption efficiencies calculated were in accordance with the results found in the literature.

[51] Regarding the chemical composition, the mass scattering efficiency of the different aerosol constituents in the PM_{10} fraction were also calculated applying the MLR method. Among all the species considered, SO_4^{2-}nm exhibited the largest mass scattering efficiency (7 ± 1 m^2g^{-1}) and dust aerosols presented the lowest mass scattering efficiency (0.2 ± 0.3 m^2g^{-1}), a value considerably lower if compared with the literature. The α_{sca} obtained for OM+EC particles was similar to the values reported for OM particles.

[52] Finally, we applied the MLR method with the absorption coefficient as the independent variable but no satisfactory results were obtained. Only C_{nm} particles correlated well with the absorption coefficient so α_{abs} were determined with a simple linear fit. This fact suggests that the absorption process was mainly dominated by carbonaceous particles and that other species did not contribute significantly.

[53] It is important to highlight that the MLR technique is useful for computing mass efficiencies and that the data requirements are not very restrictive. However, the method itself could contribute to the large variability obtained. On the other hand, the measurement method is the simplest one but the mass scattering and absorption efficiencies obtained with this technique only represent average conditions for the sampling periods. The mass scattering and absorption efficiencies obtained in this study can be used to estimate the scattering and absorption coefficients and, hence, the radiative effect of the aerosol particles.

[54] **Acknowledgments.** This work was supported by the Spanish Ministry of Science and Technology through projects CGL2008-01330-E/CLI (Spanish Lidar Network), CGL2010–18782 and CSD2007–00067; by the Andalusian Regional Government through projects P10-RNM-6299 and P08-RNM-3568; and by EU through ACTRIS project (EU INFRA-2010-1.1.16–262254).

References

Amato, F., M. Pandolfi, M. Viana, X. Querol, A. Alastuey, and T. Moreno (2009), Spatial and chemical patterns of PM_{10} in road dust deposited in urban environment, *Atmos. Environ.*, *43*, 1650–1659, doi:10.1016/j.atmosenv.2008.12.009.

Anderson, T. L., and J. A. Ogren (1998), Determining aerosol radiative properties using the TSI 3563 integrating nephelometer, *Aerosol Sci. Technol.*, *29*, 57–69, doi:10.1080/02786829808965551.

Andreae, T. W., M. O. Andreae, and C. Ichoku (2002), Light scattering by dust and anthropogenic aerosol at a remote site in the Negev Desert, Israel, *J. Geophys. Res.*, *107*(D2), 4008, doi:10.1029/2001JD900252.

Andreae, M. O., O. Schmid, H. Yang, D. Chand, J. Z. Yu, L. Zeng, and Y. Zhang (2008), Optical properties and chemical composition of the atmospheric aerosol in urban Guangzhou, China, *Atmos. Environ.*, *42*, 6335–6350, doi:10.1016/j.atmosenv.2008.01.030.

Baron, P. A., and K. Willeke (2001), *Aerosol Measurement: Principles, Techniques and Applications*, John Wiley, Hoboken, N. J.

Bond, T. C., and R. W. Bergstrom (2006), Light absorption by carbonaceous particles: An investigative review, *Aerosol Sci. Technol.*, *40*(1), 27–67, doi:10.1080/02786820500421521.

Bryant, C., K. Eleftheriadis, J. Smolik, V. Zdimal, N. Mihalopoulos, and I. Colbeck (2006), Optical properties of aerosols over the eastern Mediterranean, *Atmos. Environ.*, *40*, 6229–6244, doi:10.1016/j.atmosenv.2005.06.009.

Charlson, R. J., T. L. Anderson, and H. Rodhe (1999), Direct climate forcing by anthropogenic aerosols: Quantifying the link between atmospheric sulphate and radiation, *Contrib. Atmos. Phys.*, *72*, 79–94.

Cheng, Y. F., et al. (2008), Aerosol optical properties and related chemical apportionment at Xinken in Pearl River Delta of China, *Atmos. Environ.*, *42*, 6351–6372, doi:10.1016/j.atmosenv.2008.02.034.

Chow, J. C., J. G. Watson, D. H. Lowenthal, and L. W. Richards (2002), Comparability between $PM_{2.5}$ and particle light scattering measurements, *Environ. Monit. Assess.*, *79*, 29–45, doi:10.1023/A:1020047307117.

Drever, J. J. (1982), *The Geochemistry of Natural Waters*, 437 pp., Prentice-Hall, Englewood Cliffs, N. J.

Formenti, P., et al. (2001), Physical and chemical characteristics of aerosols over the Negev Desert (Israel) during summer 1996, *J. Geophys. Res.*, *106*(D5), 4871–4890, doi:10.1029/2000JD900556.

Forster, P., et al. (2007), Changes in Atmospheric Constituents and in radiative forcing, in *Climate Change 2007: The Physical Science Basis. Contribution of Working Group I to the Fourth Assessment Report of the Intergovernmental Panel on Climate Change*, edited by S. Solomon et al., pp. 131–217, Cambridge Univ. Press, New York.

Hand, J. L., and W. C. Malm (2007), Review of aerosol mass scattering efficiencies from ground-based measurements since 1990, *J. Geophys. Res.*, *112*, D16203, doi:10.1029/2007JD008484.

Hand, J. L., S. M. Kreidenweis, J. Slusser, and G. Scott (2004), Comparisons of aerosol optical properties derived from Sun photometry to estimates inferred from surface measurements in Big Bend National Park, Texas, *Atmos. Environ.*, *38*, 6813–6821, doi:10.1016/j.atmosenv.2004.09.004.

Jung, J., H. Lee, Y. J. Kim, X. Liu, Y. Zhang, M. Hu, and N. Sugimoto (2009), Optical properties of atmospheric aerosols obtained by in situ and remote measurements during 2006 Campaign of Air Quality Research in Beijing (CAREBeijing-2006), *J. Geophys. Res.*, *114*, D00G02, doi:10.1029/2008JD010337.

Kirchstetter, T. W., T. Novakov, and P. V. Hobbs (2004), Evidence that the spectral dependence of light absorption by aerosols is affected by organic carbon, *J. Geophys. Res.*, *109*, D21208, doi:10.1029/2004JD004999.

Kopp, R. E., and D. L. Mauzerall (2010), Assessing the climate benefits of black carbon mitigation, *Proc. Natl. Acad. Sci. U. S. A.*, *107*, 11,703–11,708, doi:10.1073/pnas.0909605107.

Lowenthal, D. H., C. F. Rogers, P. Saxena, J. G. Watson, and J. C. Chow (1995), Sensitivity of estimated light extinction coefficients to model assumptions and measurement errors, *Atmos. Environ.*, *29*, 751–766, doi:10.1016/1352-2310(94)00340-Q.

Lyamani, H., F. J. Olmo, and L. Alados-Arboledas (2008), Light scattering and absorption properties of aerosol particles in the urban environment of Granada, Spain, *Atmos. Environ.*, *42*, 2630–2642, doi:10.1016/j.atmosenv.2007.10.070.

Lyamani, H., F. J. Olmo, and L. Alados-Arboledas (2010), Physical and optical properties of aerosols over an urban location in Spain: Seasonal and diurnal variability, *Atmos. Chem. Phys.*, *10*, 239–254, doi:10.5194/acp-10-239-2010.

Malm, W. C., and J. L. Hand (2007), An examination of the physical and optical properties of aerosols collected in the IMPROVE program, *Atmos. Environ.*, *41*, 3407–3427, doi:10.1016/j.atmosenv.2006.12.012.

Müller, T., et al. (2011), Characterization and intercomparison of aerosol absorption photometers: Result of two intercomparison workshops, *Atmos. Meas. Tech.*, *4*, 245–268.

Navas-Guzmán, F., J. A. Bravo-Aranda, M. J. Granados, J. L. Guerrero-Rascado, and L. Alados-Arboledas (2010), Study of the planetary boundary layer top with Raman lidar, in *RECTA 2010, Granada (Spain)*, edited by L. Alados Arboledas et al., pp. C9-1–C9-6, Univ. de Granada, Granada, Spain.

Nessler, R., E. Weingartner, and U. Baltensperger (2005), Effect of humidity on aerosol light absorption and its implications for extinction and the single scattering albedo illustrated for a site in the lower free troposphere, *J. Aerosol Sci.*, *36*, 958–972, doi:10.1016/j.jaerosci.2004.11.012.

Ouimette, J. R., and R. C. Flagan (1982), The extinction coefficient of multicomponent aerosols, *Atmos. Environ.*, *16*, 2405–2419, doi:10.1016/0004-6981(82)90131-7.

Pandolfi M., M. Cusack, A. Alastuey and X. Querol (2011), Variability of aerosol optical properties in the Western Mediterranean Basin, *Atmos. Chem. Phys.*, *11*, 8189–8203.

Pereira, S. N., F. Wagner, and A. M. Silva (2008), Scattering properties and mass concentration of local and long range transported aerosols over the south western Iberian Peninsula, *Atmos. Environ.*, *42*, 7623–7631, doi:10.1016/j.atmosenv.2008.06.008.

Pereira, S. N., F. Wagner, and A. M. Silva (2011), Seven years of measurements of aerosol scattering properties, near the surface, in the southwestern Iberia Peninsula, *Atmos. Chem. Phys.*, *11*, 17–29, doi:10.5194/acp-11-17-2011.

Pérez, N., J. Pey, X. Querol, A. Alastuey, J. M. López, and M. Viana (2008), Partitioning of major and trace components in PM10–PM2.5–PM1 at an urban site in Southern Europe, *Atmos. Environ.*, *42*, 1677–1691, doi:10.1016/j.atmosenv.2007.11.034.

Pérez, N., J. Pey, M. Cusack, C. Reche, X. Querol, A. Alastuey, and M. Viana (2010), Variability of particle number, black carbon, and PM_{10}, $PM_{2.5}$, and PM_1 levels and speciation: Influence of road traffic emissions on urban air quality, *Aerosol Sci. Technol.*, *44*, 487–499, doi:10.1080/02786821003758286.

Petzold, A., and M. Schönlinner (2004), Multi-angle absorption photometry—A new method for the measurement of aerosol light absorption and atmospheric black carbon, *J. Aerosol Sci.*, *35*, 421–441, doi:10.1016/j.jaerosci.2003.09.005.

Pey, J., S. Rodríguez, X. Querol, A. Alastuey, T. Moreno, J. P. Putaud, and R. Van Dingenen (2008), Variations of urban aerosols in the western Mediterranean, *Atmos. Environ.*, *42*, 9052–9062, doi:10.1016/j.atmosenv.2008.09.049.

Putaud, J. P., et al. (2010), A European aerosol phenomenology-3: Physical and chemical characteristics of particulate matter from 60 rural, urban, and kerbside sites across Europe, *Atmos. Environ.*, *44*, 1308–1320, doi:10.1016/j.atmosenv.2009.12.011.

Querol, X., et al. (2004), Speciation and origin of PM_{10} and $PM_{2.5}$ in Spain, *J. Aerosol Sci.*, *35*, 1151–1172, doi:10.1016/j.jaerosci.2004.04.002.

Querol, X., et al. (2008), Spatial and temporal variations in airborne particulate matter (PM_{10} and $PM_{2.5}$) across Spain 1999–2005, *Atmos. Environ.*, *42*, 3964–3979, doi:10.1016/j.atmosenv.2006.10.071.

Querol, X., A. Alastuey, J. Pey, M. Cusack, N. Pérez, N. Mihalopoulos, C. Theodosi, E. Gerasopoulos, N. Kubilay, and M. Kocak (2009), Variability in regional background aerosols within the Mediterranean, *Atmos. Chem. Phys.*, *9*, 4575–4591, doi:10.5194/acp-9-4575-2009.

Quinn, P. K., T. L. Miller, T. S. Bates, J. A. Ogren, E. Andrews, and G. E. Shaw (2002), A 3-year record of simultaneously measured aerosol chemical and optical properties at Barrow, Alaska, *J. Geophys. Res.*, *107*(D11), 4130, doi:10.1029/2001JD001248.

Ramanathan, V., and G. Carmichael (2008), Global and regional climate changes due to black carbon, *Nat. Geosci.*, *1*, 221–227, doi:10.1038/ngeo156.

Rodríguez, S., X. Querol, A. Alastuey, and E. Mantilla (2002), Origin of high PM_{10} and TSP concentrations in summer in eastern Spain, *Atmos. Environ.*, *36*, 3101–3112, doi:10.1016/S1352-2310(02)00256-X.

Saha, A., M. Mallet, J. C. Roger, P. Dubuisson, J. Piazzola, and S. Despiau (2008), One year measurements of aerosol optical properties over an urban coastal site: Effect on local direct radiative forcing, *Atmos. Res.*, *90*, 195–202, doi:10.1016/j.atmosres.2008.02.003.

Schuster, G. L., O. Dubovik, and B. N. Holben (2006), Angstrom exponent and bimodal aerosol size distributions, *J. Geophys. Res.*, *111*, D07207, doi:10.1029/2005JD006328.

Seinfeld, J. H., and S. N. Pandis (1998), *Atmospheric Chemistry and Physics: From Air Pollution to Climate Change*, 1326 pp., John Wiley, Hoboken, N. J.

Turpin, B. J., P. Saxena, and E. Andrews (2000), Measuring and simulating particulate organics in the atmosphere: Problems and prospects, *Atmos. Environ.*, *34*, 2983–3013, doi:10.1016/S1352-2310(99)00501-4.

Vasconcelos, L. A. P., E. S. Macias, P. H. McMurry, B. J. Turpin, and W. H. White (2001), A closure study of extinction apportionment by

multiple regression, *Atmos. Environ.*, *35*, 151–158, doi:10.1016/S1352-2310(00)00273-9.

Virkkula, A., J. Backman, P. P. Aalto, M. Hulkkonen, L. Riuttanen, T. Nieminen, M. dal Maso, L. Sogacheva, G. de Leeuw, and M. Kulmala (2011), Seasonal Cycle, size dependencies, and source analyses of aerosol optical properties at the SMEAR II measurement station in Hyytiälä, Finland, *Atmos. Chem. Phys.*, *11*, 4445–4468, doi:10.5194/acp-11-4445-2011.

Vrekoussis, M., E. Liakakou, M. Koçak, N. Kubilay, K. Oikonomou, J. Sciare, and N. Mihalopoulos (2005), Seasonal variability of optical properties of aerosols in the eastern Mediterranean, *Atmos. Environ.*, *39*, 7083–7094, doi:10.1016/j.atmosenv.2005.08.011.

Wagner, F., et al. (2009), Properties of dust aerosol particles transported to Portugal from the Sahara desert, *Tellus, Ser. B*, *61*, 297–306.

White, W. H. (1986), On the theoretical and empirical basis for apportioning extinction by aerosols: A critical review, *Atmos. Environ.*, *20*, 1659–1672, doi:10.1016/0004-6981(86)90113-7.

White, W. H., and E. S. Macias (1987), On measurement error and the empirical relationship of atmospheric extinction to aerosol composition in the non-urban West, in *Visibility Protection: Research and Policy Aspects*, edited by P. S. Bhardwaja, pp. 783–794, Air Pollut. Control Assoc., Pittsburgh, Pa.

White, W. H., E. S. Macias, R. C. Nininger, and D. Schorran (1994), Size-resolved measurements of light scattering by ambient particles in the southwestern U.S, *Atmos. Environ.*, *28*, 909–921, doi:10.1016/1352-2310(94)90249-6.

World Meteorological Organization (2003), Aerosol measurement procedures guidelines and recommendations, *GAW Rep. 153*, 72 pp., Geneva, Switzerland.

Yan, H. (2007), Aerosol scattering properties in northern China, *Atmos. Environ.*, *41*, 6916–6922, doi:10.1016/j.atmosenv.2007.04.052.

Zieger, P., et al. (2011), Comparison of ambient aerosol extinction coefficients obtained from in-situ, MAX-DOAS and LIDAR measurements at Cabauw, *Atmos. Chem. Phys.*, *11*, 2603–2624, doi:10.5194/acp-11-2603-2011.

L. Alados-Arboledas, I. Foyo-Moreno, and G. Titos, Departamento de Física Aplicada, Universidad de Granada, Avda. Fuentenueva s/n, E-18071 Granada, Spain. (gtitos@ugr.es)

A. Alastuey and X. Querol, IDÆA, Department of Geosciences, CSIC, c/Jordi Girona 18-26, E-08028 Barcelona, Spain.

H. Lyamani, Centro Andaluz de Medio Ambiente, Universidad de Granada, Avda. del Mediterráneo s/n, E-18006 Granada, Spain.